93   Final

A Multi-branched Model of the Cardiovas-
cular System: Application to G-research

Sherwood Samn

Armstrong Laboratory (AFMC)
Aerospace Medicine Directorate
Clinical Sciences Division
Brooks AFB TX   78235-5117

AL/AO-PC-1993-0034

Heretofore cardiovascular system (CVS) models have been either too refined with
applications only to special subsystems of the CVS, or too gross with only limited
versatility due to their inadequate resolution. In this paper, we report on a
multi-branched model of the complete CVS that bridges the gap between these two
groups of models. This model, which is motivated by aviation and space research,
extends the models of Avolio and Jaron.

Cardiovascular system; model; hemodynamics; acceleration.

8

Unclassified   Unclassified   Unclassified   UL

A MULTI-BRANCHED MODEL OF THE CARDIOVASCULAR SYSTEM: APPLICATION TO G-RESEARCH

SHERWOOD SAMN

Armstrong Laboratory (AFMC)
Aerospace Medicine Directorate
Clinical Sciences Division
Brooks AFB, TX 78235-5117

Accesion For		
NTIS CRA&I		X
DTIC TAB		
Unannounced		
Justification		
By		
Distribution /		
Availability Codes		
Dist	Avail and/or Special	
A-1		

ABSTRACT

Heretofore cardiovascular system (CVS) models have been either too refined with applications only to special subsystems of the CVS, or too gross with only limited versatility due to their inadequate resolution. In this paper, we report on a multi-branched model of the complete CVS that bridges the gap between these two groups of models. This model, which is motivated by aviation and space research, extends the models of Avolio and Jaron.

KEYWORDS

Cardiovascular system; model; hemodynamics; acceleration.

INTRODUCTION

Aircrew loss of consciousness (LOC) in high-performance aircraft due to G-stress is of obvious concern to the military aviator. Anti-G measures to minimize this risk can be evaluated and designed with the help of mathematical models of the cardiovascular system (CVS). What may not be as evident is applying some of these models to predict the vulnerability of certain subclinical cardiovascular disorders (e.g. mitral valve prolapse) to G-stress in flying. Improved modeling can lead to more objective guidelines for the selection and retention of pilots.

Modeling the partial or complete cardiovascular systems has been attempted by many investigators over the last three decades. To review these models here would be unnecessary because there are already many excellent reviews in the literature. Most of the models up to now have been too refined, addressed only a portion (for example, the arterial tree) of the CVS, or, if they do address the complete CVS, have been rather gross.

Because feedback controls inherent in the CVS play important roles in G-research, we must necessarily

1

consider a holistic CVS model. With the advent of more powerful computers, the computational burden associated with a refined holistic model, which is still nontrivial, is now less of a problem.

The model reported here is basically an extension of two models: Avolio [1] and Jaron [2]. Avolio's model is an arterial model that takes into account the major architectural features of the arterial tree. This model in turn is based on the one developed by the group at the University of Pennsylvania headed by Noordergraff [3]. Jaron's model is a holistic model that emphasizes G-stress with provisions for straining maneuvers, anti-G suits, and positive pressure breathing. This model in turn evolved largely from the works of Snyder and Rideout [4, 5]. Recently Sud [6] also embeds multi-branched arterial and venous trees into a holistic model. He uses a novel finite-element approach. Our approach here is more conventional.

METHODOLOGY

As our model is an extension of Jaron's [2] using Avolio's arterial tree [1], we refer readers to their works for details. We will only describe those features we have added or modified.

Starting from Avolio's arterial tree [1], we made some modifications to its branch names, its parameter values, and its structure, so that it conforms more closely to the actual anatomy. We also embedded the tree in three-dimensional space to model the direction of the G-force more realistically.

Analysis of an early version of the model indicates that it behaves much better numerically when the mean radius of an arterial segment is assumed to be a monotone decreasing function of its distance from the heart. We have made this assumption and fitted the radii given in [1] by an exponentially decreasing function. A similar approach was used by Anliker [7] in his distributed arterial model.

In lumped models of the arterial system, it is customary to model an arterial segment by an L-network (See the theoretical justification for this was given by Rideout and Dick [4]). By simplifying the Navier-Stokes and continuity equations and equations for vessel wall movement, they arrived at the following equations governing the pressures and flows in an arterial segment:

$$\dot{f}_m = \frac{1}{L_m}\left(p_{mi} - p_{mo} - R_m f_m\right) \tag{1}$$

$$\dot{p}_m = \frac{1}{C_m}\left(f_{mi} - f_{mo}\right) \tag{2}$$

Here f and p denote respectively flow and pressure. The subscripts mi, m, and mo denote respectively the locations at the entrance, middle, and exit of the m-th arterial segment. The parameters R_m, C_m, and L_m are given by

$$R_m = \frac{8\mu l_m}{\pi r_m^4} \tag{3}$$

$$C_m = \frac{3\pi l_m}{2E_m h_m} r_m^3 \tag{4}$$

$$L_m = \frac{2\rho l_m}{\pi r_m^2} \tag{5}$$

where ρ is the fluid density, μ the coefficient of viscosity, E_m, h_m, and l_n are respectively the Young modulus of elasticity, the thickness of the vessel wall, and the length of the m-th arterial segment.

Making the (informal) substitutions $p_{mi} = p_{m-1}$, $p_{mo} = p_m$, $f_{mi} = f_m$, and $f_{mo} = f_{m+1}$ in the above equations, one arrives at a new set of equations:

$$\dot{f}_m = \frac{1}{L_m}\left(p_{m-1} - p_m - R_m f_m\right) \tag{6}$$

$$\dot{p}_m = \frac{1}{C_m}\left(f_m - f_{m+1}\right) \tag{7}$$

This is the L-network that has been adopted in most of today's models. A more rigorous treatment can be made to arrive at a similar set of equations except now the parameters R_m and L_m will depend not only on properties of the m-th segment, but also on that of the (m-1)-th segment. This shortcoming can be avoided by using a more symmetric T-network formulation described by the following equations:

$$\dot{f}_{mi} = \frac{2}{L_m}\left(p_{mi} - p_m - \frac{R_m}{2}f_{mi}\right) \tag{8}$$

$$\dot{f}_{mo} = \frac{2}{L_m}\left(p_m - p_{mo} - \frac{R_m}{2}f_{mo}\right) \tag{9}$$

$$\dot{p}_m = \frac{1}{C_m}\left(f_{mi} - f_{mo}\right) \tag{10}$$

This model is essentially the one we used for our arterial segments. Because the parameters in this set of equations depend only on properties associated with the m-th segment, the T-network formulation is more natural in modeling the arterial segments at bifurcations.

To account for the energy loss due to viscoelastic properties of the vessel wall, Jaron added a term to the last equation and obtained:

$$\dot{p}_m = \frac{1}{C_m}\left(f_{mi} - f_{mo}\right) + R_{m,el}\left(\dot{f}_{mi} - \dot{f}_{mo}\right) \tag{11}$$

The parameter $R_{m,el}$ is chosen to be inversely proportional to C_m: $R_{m,el} = K_{el}^a/C_m$, where the arterial energy-loss constant K_{el}^a is a system parameter independent of the segment number m.

In implementing the venous system, we assume, for simplicity, that its topology is identical to that of the arterial system. For a more accurate simulation, the geometry of branches near the heart (especially, the inferior and superior vena cava) will need to be redefined. For each venous segment, we assume its mean radius is larger, by a constant factor, than its counterpart in the arterial system, while its Young modulus is smaller, also by a constant faster, than its counterpart. Because of lower pressure in the veins as well as vessel wall makeup, the veins are susceptible to collapse. To take this possibility into account, we assume that, when the transmural pressure becomes negative and a venous segment experiences collapse, that the flow resistance in this segment, R_m, increases according to the relation:

$$R_m = \frac{8\mu l_m r_{mo}^2}{\pi r_m^6} \tag{12}$$

3

where r_{mo} is the assumed radius of the m-th segment when the transmural pressure is zero. It is also customary [5, 2] to increase the capcitance C_m by a factor of 20 during venous collapse when the transmural pressure becomes negative. However, we have not implemented this factor in our early runs.

Following Jaron, we connect each terminal branch of the arterial tree to its counterpart in the venous tree by a peripheral compartment whose dynamics can be described by the equations:

$$f_{pa} = (p_a - p_p)/R_a \tag{13}$$

$$f_{pv} = (p_p - p_v)/R_v \tag{14}$$

$$\dot{p}_p = \frac{1}{C_p}(f_{pa} - f_{pv}) \tag{15}$$

Here, p_a and p_v are the pressures in corresponding terminal branches in the arterial and venous tree respectively, and p_p is the peripheral pressure. The peripheral flows, f_{pa} and f_{pv}, come in from the arterial side and go out to the venous side, respectively. The parameters R_a and R_v are the peripheral resistances, and C_p is the peripheral capacitance.

The basic model we have implemented has 135 arterial, 135 venous, and 61 peripheral segments. However, these numbers can be easily increased by specifying a maximum allowable length for each segment in the system. Because most of the parameters in the model are defined in terms of segment length, the model can be refined (shorter segments) without much change. In theory, segment lengths can be made to approach the grid size typically used in computational fluid dynamics. The only limitation would be the size of the computer memory.

In smaller CVS models where the total number of compartments are less than, say, fifty, most researchers have integrated the associated system of ordinary differential equations using some variants of the Euler's method. For our larger model here, we need an efficient stiff differential equations solver. Fortunately, such a solver (LSODES from ODEPACK) is already available (from *NETLIB*).

While experimenting with the new model, we found that it is very sensitive to initial conditions. To establish the stability of the model, we devise the following method to obtain, indirectly, stable initial conditions by putting the model through three transient- and instability-removing phases. The first phase consists of running the CVS model with a simplified arterial-peripheral-venous system (APVS) that we will call the simplied model and is basically Jaron's model. The purpose of this phase is to remove transients in the simplified model. In the second phase, still running the simplified model (with its smaller APVS), the aortic and vena cava pressures are continually passed to the full APVS (with its 331 branches), which begins to run in parallel with the simplified model. Initially, the full APVS is assumed to be in hydrostatic equilibrium. In the third and final phase, the simplified APVS is totally replaced by the full APVS which means that the aortic flow and the vena cava flow are no longer taken from the simplified APVS, but from the full APVS. By using this method, we are able to stabilize the full model without having to specify exactly what the initial conditions are.

In tuning model parameters to match experimental data, one of our goals is to keep the number of adjustable parameters down to a minimum. Even though there are 331 compartments in the basic APVS, we basically adjusted only six parameters to get the results reported in the next section. They are the three peripheral parameters, R_a, R_v, and C_p, the two energy-loss constants, K_{el}^a and K_{el}^r, for the arterial and venous system respectively, and P_o^a, the initial aortic pressure when the arterial system is in hydrostatic equilibrium. (Since the vena cava pressure usually remains small, it is given a fixed value.) In smaller CVS

models, peripheral parameters are generally different for different peripheral compartment. In our case it is impractical, especially during this early stage of model development, to try to assign different parameters to (61) different peripheral compartments, since most of the values are unknown anyway. We have therefore chosen to use the same set of peripheral parameter values for R_a, R_v, and C_p for all compartments. Numerical stability of the model is sensitive to the energy-loss constants K_{el}^a and K_{el}^v. When their values are large, in effect making the arterial and venous segment rigid, the numerical integration is stable and fast. As we decrease the values of these parameters, in effect making the segments more elastic, the numerical integration becomes slower and eventually becomes unstable. The final parameter, P_o^a, has the effect of preconditioning the arterial system. Larger value of this parameter will lead to larger mean arterial pressures.

While builders of most CVS models stress models portability and short run times, probably for pedagogical reasons, our emphasis here is on neither, mainly because we view our model as a special tool for a relatively narrow field of research. With no concerted effort to optimize the code, the model currently requires, on the average, approximately 6 hours on a VAX/8650 and less than 5 minutes on a Cray-2 to make a run of 50 heart beats, using less than a megaword. These times actually change according to the stiffness of the equations, which in turn depends on the parameters of the model. The size of this model is very small compared to other fluid mechanics models that literally solve millions of equations.

RESULTS/DISCUSSION

We report here some of the results obtained during the development of this model relating to parameter estimation, model validation, and model prediction. All simulation runs used the G-profile shown in Figure 1, an actual G-profile from centrifuge experiments.

Parameter Estimation. The six parameters in the model mentioned above were adjusted, by trial and error, so that the new model results match approximately those of Jaron's model. Figures 3 and 4 provide a comparison of the aortic pressures obtained from Jaron's model and the new model respectively. While qualitatively similar, they differ quantitatively in some details. Work is underway to determine (from real data) which features in the new results are artifacts and to make appropriate adjustments in the model. The fact that these results were obtained by adjusting only 6 parameters is very encouraging. The vena cava flows predicted by Jaron's model and the new model (Figure 2) are quite different. This variance could probably be accounted for by the simplifying assumption, made in the new model, that the geometric structure of the vena cava is similar to that of the ascending aorta.

Model Validation. We do not have humans centrifuge blood flow data with which to compare our model results, we used instead some of the centrifuge data for a baboon collected recently by Dr. David Self of the Armstrong Laboratory. Figures 5 and 6 show aortic flows from a baboon and from the new model respectively. Because baboon and human physiology are different, we only expect qualitative similarities in the two. In this case, an increase in heart rate and a decrease in stroke volume during the high-G plateau are noticeable in both. These similarities give some credence to our model.

Model Prediction. One reason for building a 3-dimensional model is to investigate the effects of body position on blood flow under high-G or, more generally, under varying G, both in magnitude and in direction. Figures 7 and 8 show pressures at 7 different locations along the carotid artery respectively for two different body positions: standing (straight) and sitting (with legs extended forward), again under the same

G-profile mentioned above. The direction of the G-force is constant (head to toe). The difference between carotid pressures, indices for tunneled vision, blackout, and loss of consciousness, for the two different body positions is evident though not unexpected. The important point we want to make with these simulations is not so much that carotid pressure changes with body position, but that a 3-dimensional model, like the model here, can and should be used to simulate realistic G-profiles like those encountered in parabolic flights.

CONCLUSION

We have implemented multi-branched arterial, peripheral, and venous models into a holistic model [2] to study G-stress. While the model is new, it is based on many previous works and its predictions, especially of arterial variables, seem reasonable. However, like almost all models, further improvements and extensions can be made, especially when more human data become available. Because it is 3-dimensional, this model can better take advantage of real world data; it not only simulates changing pilot posture, but also changing G-force (magnitude and direction). Using high technology tools, researchers are now collecting quality human physiological data in flight as well as in the centrifuge. With human centrifuge data, we can improve our model and promote better understanding of human physiology under altered G.

References

[1] Avolio, A. P. (1980). Multi-branched model of the human arterial system, Med. & Biol. Eng. & Comput., Vol. 13, pp. 709-718.

[2] Jaron, D., Moore, T. W., and Bai, J. (1988). Cardiovascular Responses to Acceleration Stress: A Computer Simulation, Proc. of the IEEE, Vol. 76, pp. 700-707.

[3] Noordergraaf, A. (1963). An analog computer for the human systemic circulatory system, in A. Noordergraaf, G. N. Jager, and N.Westerhoff (eds.), Circulatory Analog Computers, North Holland Publishing Co., Amsterdam.

[4] Rideout, V. C. and Dick, D. E. (1967). Difference-Differential Equations for Fluid Flow in Distensible Tubes. IEEE Trans. Biomed. Eng., Vol. BME-14, no.4, pp. 171-177.

[5] Snyder, M. F. and Rideout, V. C. (1969). Computer Simulation Studies of the Venous Circulation. IEEE Trans. Biomed. Eng., Vol. BME-16, No. 4, pp. 325-334.

[6] Sud, V. K., Srinivasan, R. S., Charles, J. B., and Bungo, M. W. (1992). Mathematical modelling of flow distribution in the human cardiovascular system. Med.& Biol. Eng. & Comput., Vol. 30, pp.311-316.

[7] Anliker, M., Rockwell, R. L., and Ogden, E. (1971). Nonlinear Analysis of Flow Pulses and Shock Waves in Arteries. ZAMP, Vol. 22, pp. 217-246.
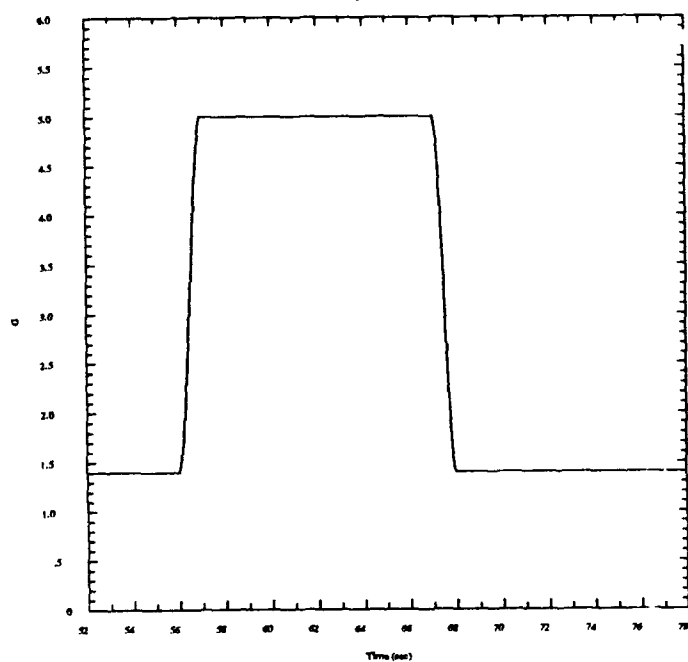
Fig. 1: G-Profile

Fig. 2: Vena Cava Flow (Antonov, BioNova M)

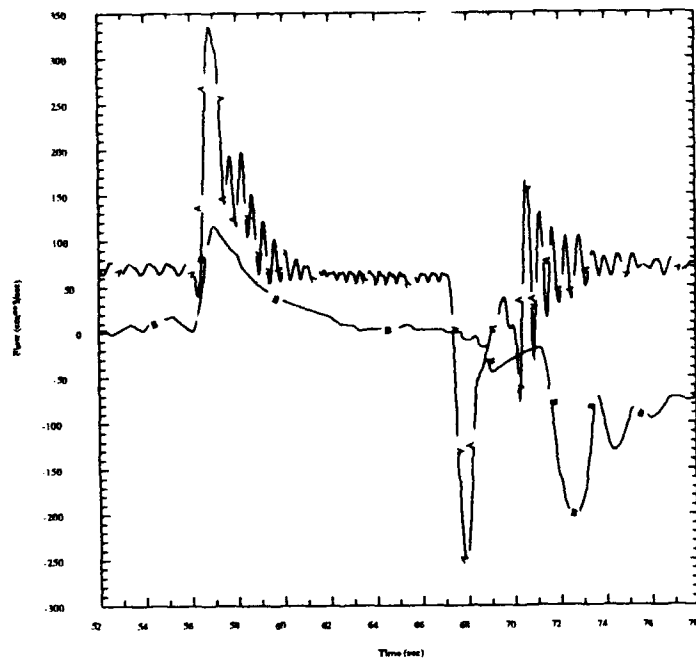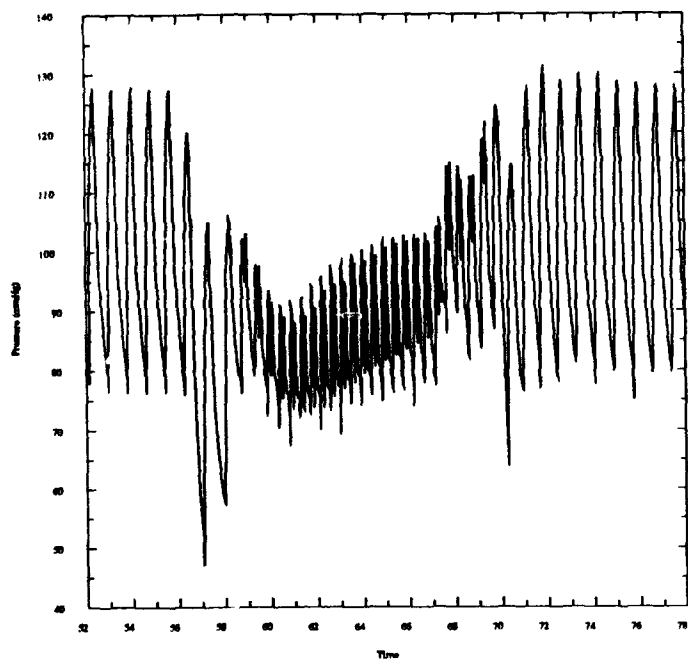
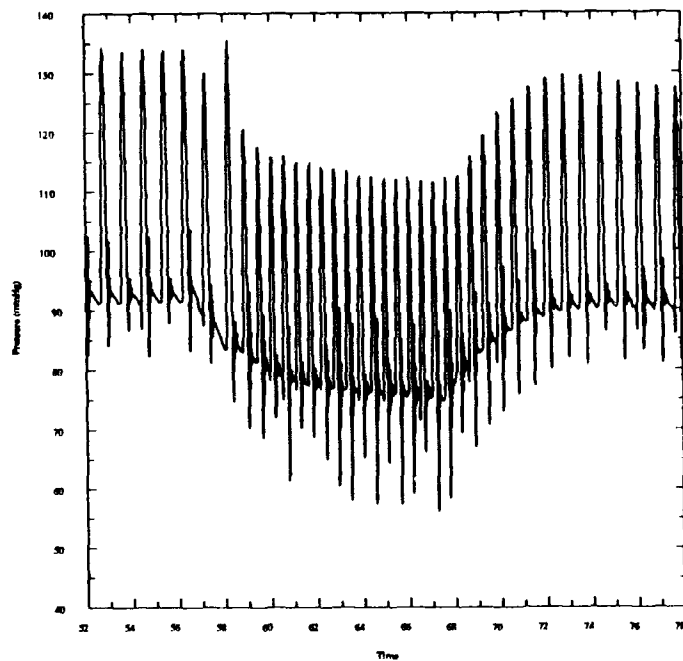Fig. 3: Aortic Pressure: Jaron Model

Fig. 4: Aortic Pressure: New Model
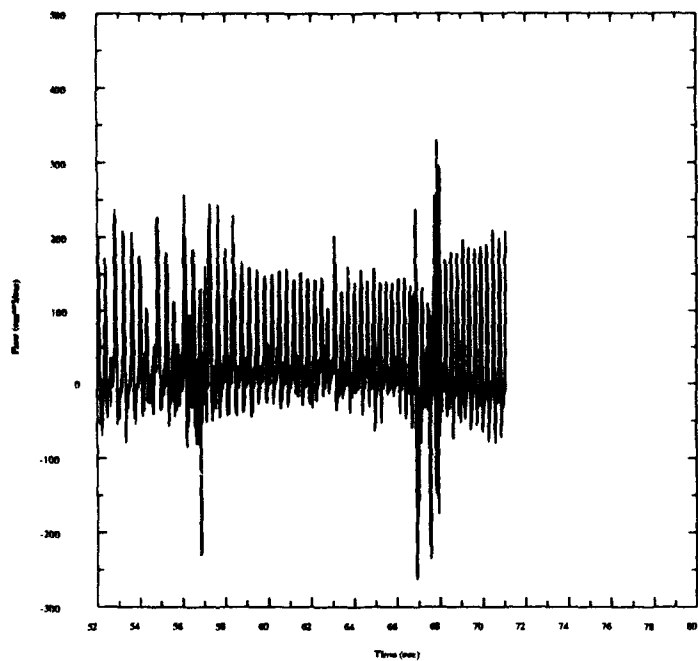
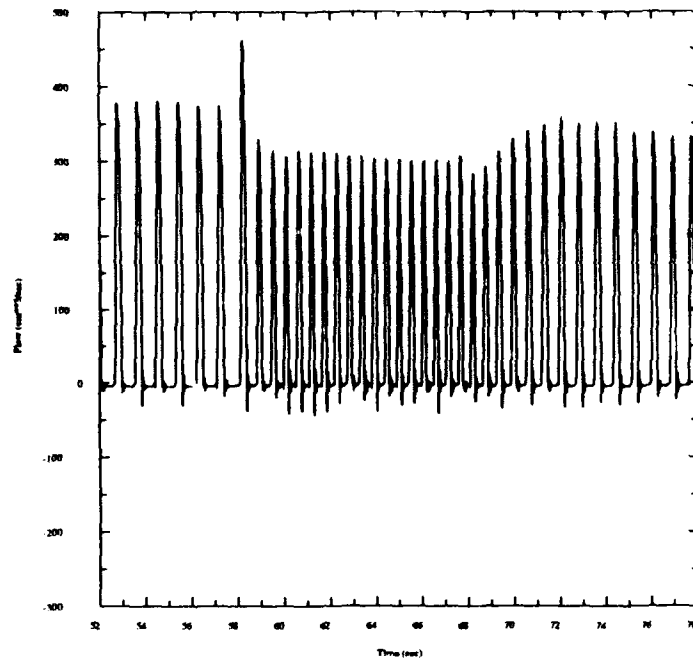Fig. 5: Dr. Self: AORTIC FLOW / Baboon
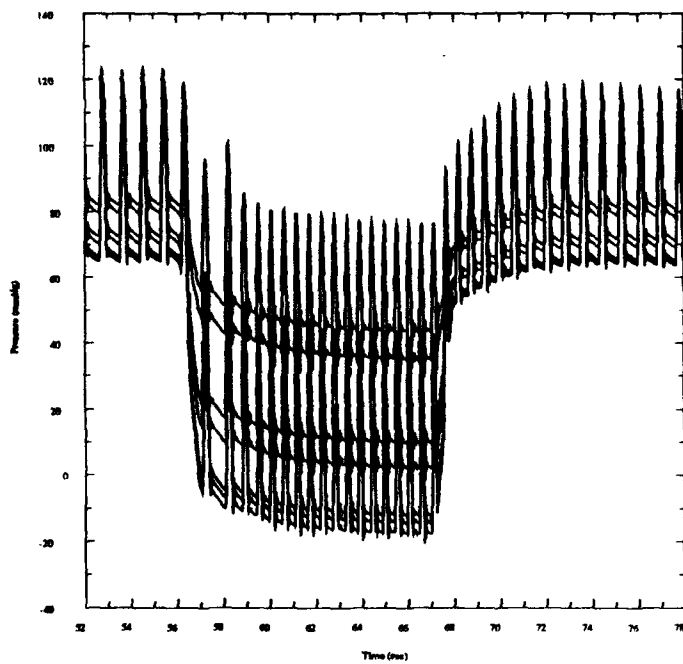
Fig. 6: Model: Aortic Flow

Fig. 7: Carotid Pressure (Standing)

Fig. 8: Carotid Pressure (Half Sitting)